Inorganic Chemistry

Article

pubs.acs.org/IC

Electronic Communication Across Diamagnetic Metal Bridges: A Homoleptic Gallium(III) Complex of a Redox-Active Diarylamido-Based Ligand and Its Oxidized Derivatives

Brendan J. Liddle,[†] Sarath Wanniarachchi,[†] Jeewantha S. Hewage,[†] Sergey V. Lindeman,[†] Brian Bennett,[‡] and James R. Gardinier*,[†]

[†]Department of Chemistry, Marquette University, Milwaukee, Wisconsin 53201-1881, United States

[‡]Department of Biophysics, Medical College of Wisconsin, Milwaukee, Wisconsin 53226, United States

Supporting Information

ABSTRACT: Complexes with cations of the type $[Ga(L)_2]^{n+}$ where L = bis(4-methyl-2-(1H-pyrazol-1-yl)phenyl)amido and n = 1, 2, 3 have been prepared and structurally characterized. The electronic properties of each were probed by electrochemical and spectroscopic means and were interpreted with the aid of density functional theory (DFT) calculations. The dication, best described as $[Ga(L^{-})(L^{0})]^{2+}$, is a Robin-Day class II mixed-valence species. As such, a broad, weak, solvent-dependent intervalence charge transfer (IVCT) band was found in the NIR spectrum in the range 6390−6925 cm^{-1}, depending on the solvent. Band shape analyses and the use of Hush and Marcus relations revealed a modest electronic coupling, H_{ab} of about 200 cm^{-1}, and a large rate constant for electron transfer, k_{et}, on the order of 10^{10} s^{-1} between redox active ligands. The dioxidized complex $[Ga(L^{0})_2]^{3+}$ shows a half-field ΔM_s = 2 transition in its solid-state X-band electron paramagnetic resonance (EPR) spectrum at 5 K, which indicates that the triplet state is thermally populated. DFT calculations (M06/Def2-SV(P)) suggest that the singlet state is 21.7 cm^{-1} lower in energy than the triplet state.

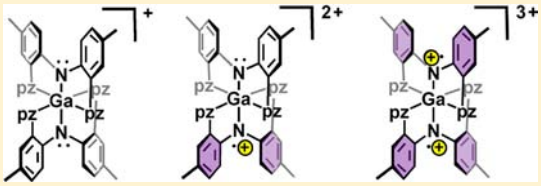

INTRODUCTION

Over the past few decades, the study of mixed-valence (MV) compounds has been pivotal for advancing comprehension of long-range electron transfer of importance to both basic biological functions and, potentially, to future molecular electronics applications.[1] A majority[2] of the MV complexes studied have been of the type M^{n+}-(bridge)-$M^{(n-1)+}$ where the bridge is an organic group such as in the Creutz-Taube ion, $[(NH_3)_5Ru^{II}(\mu\text{-pyrazine})Ru^{III}(NH_3)_5]^{5+}$.[3] There has also been a great deal of interest in purely organic systems of the type ***D*-*OB*-D$^{+\bullet}$**, where ***OB*** is an organic bridge and ***D*/*D*$^{+\bullet}$** are the one-electron redox partners of an organic donor.[4] A popular class of such organic derivatives is those with diarylamine donors that flank an organic bridge, Figure 1.[5−8] Electronic communication between donor ends of such molecules can vary dramatically by changing: (i) the groups, X, along the diarylamine donor;[5c,h−j] (ii) the type of bridge;[7a,8,9] (iii) the bridge length; or (iv) the geometric disposition of donors about the bridge,[5i,j,9] including the dihedral angle between bridging phenylene groups (that also affect the dihedral of orbitals containing the nitrogen lone pair).[10] In cases such as A and B in Figure 1, electronic communication can occur via tunneling, superexchange, or a "hopping" mechanism whereby the bridge becomes an active participant. The latter is important for longer, more highly conjugated and electron-rich bridges. Both through-bond and through-space superexchange interactions become important for short bridges such as found in the tetraanisyl-*o*-phenylenediamine cation radical.[9]

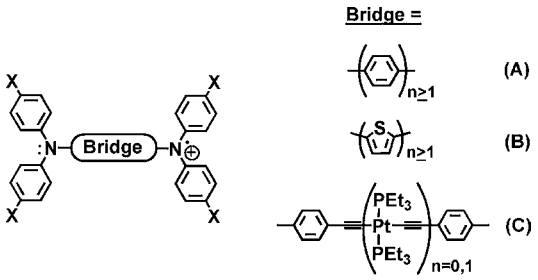

Figure 1. (A−C) Diarylamine-based mixed valent compounds.

An important class of MV complexes is one like Figure 1C (n = 1)[8] that contains organic donors separated by a metal bridge.[11] One-electron oxidized or reduced forms of metal dioxolenes,[12] dithiolenes,[13] diimines,[14−17] *o*-semiquinones,[18] *o*-iminosemiquinones,[19] polypyridyls,[20] and tridentate catecholates[21] can all fall into this category. Some important aspects of the chemistry of these and related metal complexes of redox-active ligands were the subjects of a recent special issue of *Inorganic Chemistry*[22] and of several reviews.[23] With relation to the organic derivatives mentioned above, the interjection of the $Pt(PEt_3)_2$ bridge between (di/tri)arylamine donors, Figure 1C (n = 1), permitted weak electronic coupling (H_{ab} = 350 cm^{-1})

Received: July 3, 2012
Published: November 19, 2012

between donor ends, but this coupling was weaker than that found for derivatives where a phenylene (H_{ab} = 440 cm^{-1})[5c] or a *p*-dimethoxyphenylene group (H_{ab} = 520 cm^{-1})[7a] replaces the metal bridge. Thus, despite the former possessing fewer number of sigma bonds separating donor ends (and a shorter $\mathbf{D}\cdots\mathbf{D}^{+\cdot}$ separation) than in the pure organic cases, the energetic mismatch between donor and the metal bridge has a small detrimental influence on the electron transfer.

We were interested in further examining how effectively electronic communication could be mediated by using only a single atom bridge between two diarylamido groups. In particular, we recently prepared a series of diarylamines that have a pyrazolyl group situated at an *ortho*-position of each aryl (Figure 2).

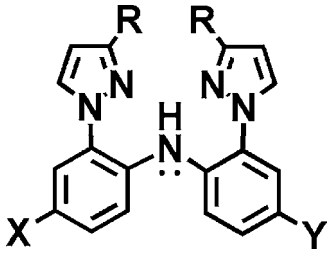

Figure 2. Di(2−3R-pyrazolyl)-*p*-arylamines, H(XY^R).

The coordination chemistry of tricarbonylrhenium(I)[24] and rhodium[25] complexes showed that these pincer-type ligands are electrochemically active and chemically noninnocent. The electronic properties and reactivity of the complexes could be predictably fine-tuned by substituting at the pyrazolyl, at the *para*-aryl positions, or even at the metal center. In those studies, only one ligand was bound to a metal center. We envisioned constructing molecular wires by assembling strings of M(L = XY^R)$_2$ complexes together to give species such as LM-[(L-L)M(L-L)]$_n$-ML (n = 0, 1, 2...). Therefore, it became of interest to examine potential electronic interactions between two ligands across a single metal ion bridge to inform future wire designs. Our investigations began with simple model complexes of redox-silent gallium(III) with the added purpose of obtaining structural and spectroscopic markers for ligand-based radicals that should also be of use in future studies that incorporate transition metals. Herein, we report on the preparation and properties of the complete valence series of $[Ga(L)_2]^{n+}$ complexes (n = 1−3).

RESULTS AND DISCUSSION

The reaction between 2 mol equivalents of "Li(L)" (formed in situ from Li(*n*-Bu) and H(L) in THF at −20 °C) and 1 mol equivalent GaI_3 gives blue-luminescent $[Ga(L)_2](I)$, rather surprisingly, as the insoluble product and LiI as the soluble product, a mixture that can be easily separated by filtration. As the signal for iodide oxidation interferes with the ligand oxidation wave in voltammetry experiments (see Supporting Information), an ensuing metathetical reaction between $[Ga(L)_2](I)$, $(\mathbf{1})(I)$, and $TlPF_6$ afforded $[Ga(L)_2](PF_6)$, $(\mathbf{1})(PF_6)$, in high yield.

Single crystals of $(\mathbf{1})(PF_6)\cdot 1.75\ CH_2Cl_2$ suitable for X-ray diffraction were grown by layering hexanes on a CH_2Cl_2 solution and allowing solvents to diffuse. The compound crystallizes with two crystallographically independent $(\mathbf{1})(PF_6)$ units. Views of the structure of one of the cations are shown in Figure 3. The gallium center in each resides in a compressed octahedral GaN_6 environment as a result of the disparate

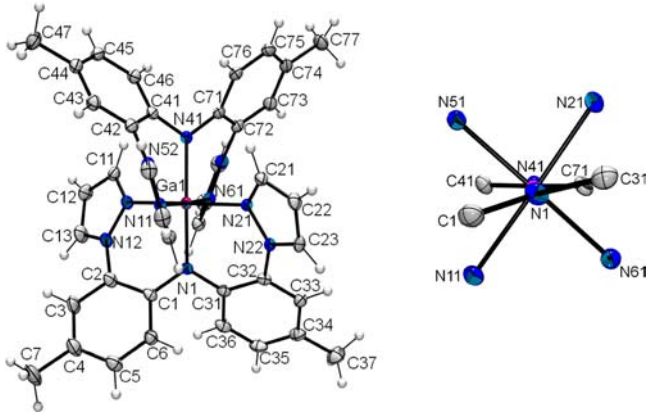

Figure 3. Views of one of the two crystallographically independent cations $[Ga(L)_2]^+$, $(\mathbf{1})+$, in the crystal of $(\mathbf{1})(PF_6)\cdot 1.5CH_2Cl_2$ (left) with a view approximately down the N1−Ga1−N41 vector showing the small dihedral angle between C1−N1−C31 and C41−N41−C71 planes. Selected bond distances (Å): Ga1−N1, 1.947(2); Ga1−N41, 1.953(2); Ga1−N11, 2.099(2); Ga1−N21, 2.094(2); Ga1−N51, 2.101(2); Ga1−N61, 2.085(2). Selected bond angles (°): N1−Ga1−N41, 179.05(11); N11−Ga1−N21, 178.60(9); N51−Ga1−N61, 177.85(9); N1−Ga1−N11, 90.00(10); N1−Ga1−N21, 89.34(9); N41−Ga1−N51, 89.08(10); N41−Ga1−N61, 88.85(10); N11−Ga1−N51, 92.93(9); N11−Ga1−N61, 86.49(10); N21−Ga1−N51, 85.85(9); N21−Ga1−N61, 94.75(9).

distances associated with the two types of Ga−N bonds. Those bonds associated with the diarylamido portion of the ligand, $Ga-N_{Ar}$, average 1.949(6) Å which is shorter than found in two independent structure determinations of a related hexacoordinate gallium(III) ONO- pincer complex Ga(dbqdi = 3,5-di-*tert*-butyl-1,2-quinone-1-(2-hydroxy-3,5-ditert-butyl-phenyl)imine)$_2$ (avg. 2.020(3) Å[21d] and avg. 2.027(3) Å[21e]). As expected, the $Ga-N_{Ar}$ bonds in the current six-coordinate complex are longer than those in three- or four-coordinate diphenylamidogallium-(III) complexes which range from 1.85 to 1.91 Å.[26] The gallium−nitrogen bonds in $(\mathbf{1})^+$ associated with pyrazolyl groups, $Ga-N_{pz}$, range from 2.085(2) Å to 2.141(3) Å and average 2.101 Å. These values are in good agreement with six-coordinate tris(pyrazolyl)borate complexes of gallium(III).[27] Notably, in $(\mathbf{1})^+$ the amido nitrogen atoms are planar with the sum of angles around each of 360°. The six-membered chelate rings (avg. $N_{pz}-Ga-N_{pz}$ bite angle, 88(1)°) are nonplanar such as to allow the diarylamido NC_2- moieties to be nearly coplanar across the gallium bridge. That is, there is a small dihedral angle of 16.6(8)° between the mean plane containing C1−N1−C31 and that containing C41−N41−C71 (Figure 3, right). Thus, the nitrogen p-orbitals containing the lone-pair electrons are expected to be roughly parallel with each other but are separated by 3.897(3) Å (avg. N···N distance). This geometry is in contrast to the case of the ONO-pincer complex, $Ga(dbqdi)_2$ whose five-member (planar) chelate rings force the two ligands to be orthogonal, with the dihedral angle of 87.05° between mean planes containing the C−N−C atoms.[21d,e]

Representative cyclic voltammograms of the free ligand, H(L), and of $(\mathbf{1})(PF_6)$ in CH_2Cl_2 are given in Figure 4, while a summary of electrochemical data of $(\mathbf{1})(PF_6)$ in three different solvents is provided in Table 1. The voltammogram of H(L) in CH_2Cl_2 shows a single irreversible oxidation wave with an

dx.doi.org/10.1021/ic301437f | *Inorg. Chem.* 2012, 51, 12720−12728

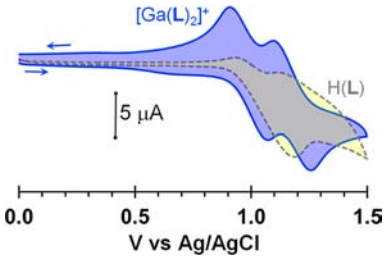

Figure 4. Overlay of cyclic voltammograms of H(L) and $(1)(PF_6)$ in CH_2Cl_2 obtained at a scan rate of 200 mV/s.

Table 1. Electrochemical Data for $(1)(PF_6)$ in Various Solvents

solvent	$E_{1/2}(1)$, V[a,b]	$E_{1/2}(2)$, V[a,b]	ΔE, V[c]	K_{com}[d]
CH_2Cl_2	0.939(3)	1.173(4)	0.184	1.39×10^3
PC[e]	0.838(2)	0.994(5)	0.156	4.62×10^2
CH_3CN	0.888(1)	1.065(1)	0.177	1.06×10^3

[a]Average values obtained for scan rates of 50, 100, 200, and 400 mV/s with 0.1 M $NBu_4(PF_6)$ as supporting electrolyte. [b]V versus Ag/AgCl. [c]$\Delta E = E_{1/2}(1) - E_{1/2}(2)$. [d]$K_{com} = e^{(\Delta E \cdot F/RT)}$, T = 295 K. [e]Propylene carbonate.

anodic peak at ca. 1.2 V versus Ag/AgCl ($i_a/i_c > 1$), whereas that of $[Ga^{III}(L^-)_2](PF_6)$ in this solvent shows two overlapping, reversible, one-electron oxidation waves at 0.94 and 1.17 V versus Ag/AgCl. Since gallium(III) cannot be oxidized to gallium(IV), the oxidation waves are unequivocally identified as ligand-based affording $[Ga^{III}(L^-)(L^0)]^{2+}$, $(2)^{2+}$, and $[Ga^{III}(L^0)_2]^{3+}$, $(3)^{3+}$, respectively. The close proximity of the two ligands connected by a one-atom spacer can give rise to two oxidation waves by simple Coulombic means and/or by electronic communication via superexchange or hopping mechanisms. Coulombic interactions do not have a spectroscopic marker, whereas electronic communication (via superexchange or hopping) leaves a signature in the form of an intravalence charge transfer (IVCT) band which is indeed observed in the current case, *vide infra*. The equilibrium constant for comproportionation according to eqs 1 and 2 is on the order of 10^2 to 10^3 (determined from the electrochemical data in various solvents, Table 1), which indicates a small but significant

$$[Ga^{III}(L^-)_2]^+ + [Ga^{III}(L^0)_2]^{3+} \leftrightarrow 2[Ga^{III}(L^-)(L^0)]^{2+} \quad (1)$$

$$K_{com} = [(2)^{2+}]^2/[(1)^+][(3)^{3+}] \quad (2)$$

degree of electronic communication in mono-oxidized $(2)^{2+}$. The relatively small value of $K_{com} \sim 10^3$ is one indicator that $(2)^{2+}$ is a Robin-Day class II mixed valent species.[3c,28]

Theoretical Studies. In order to gain further insight into the nature of the two oxidation waves and to help rationalize the other experimental properties of the oxidized species, the cations $(1)^+$, $(2)^{2+}$, and $(3)^{3+}$ were studied by density functional theory. Four models were examined (M06 or B3LYP functionals with either the LANL2DZ or Def2-SV(P) basis sets), each also accounted for solvation in dichloromethane by employing the polarizable continuum model (PCM). While all gave qualitatively similar trends, the combination (U)M06/Def2-SV(P) gave most satisfactory correlation to experimental data (bond distances and spectroscopic parameters) as summarized in the Supporting Information. The major findings of these studies are summarized below. First, despite missing solvated anions in the theoretical study, a 625 mV difference between first and second oxidation potentials was obtained which parallels the experimental finding of two separate oxidation waves. Second, for the doubly oxidized $(3)^{3+}$, the singlet diradical state was found to be 21.7 cm^{-1} lower energy than the triplet state. Third, the major structural changes along the valence series occur for Ga−N bonds (despite a lack of participating orbitals on the metal center). Thus, upon successive oxidation, the Ga−N bonds associated with the diarylamido, $Ga-N_{Ar}$, lengthen while those associated with the pyrazolyls, $Ga-N_{pz}$, shorten. The unoxidized and dioxidized complexes are more or less symmetric about gallium(III). However, the bond distances associated with each ligand of the mono-oxidized species $(2)^{2+}$ are distinct. One ligand has a longer $Ga-N_{Ar}$ bond and a shorter average $Ga-N_{pz}$ distance than the other ligand. In $(2)^{2+}$, the longer $Ga-N_{Ar}$ bond distance 2.081 Å resembles the average distance 2.043 Å calculated for the doubly oxidized complex $(3)^{3+}$, while the shorter $Ga-N_{Ar}$ distance of 1.937 Å resembles the average distance of 1.966 Å calculated for the unoxidized complex $(1)^+$. The intraligand C−C bond distances also show a similar disparity, but the differences between each ligand in $(2)^{2+}$ are much less pronounced than those distances involving gallium. Therefore, examination of the Ga−N bond distances allows one to most easily discern which ligand is oxidized. Electronically, the paramagnetic species are ligand-centered radicals with negligible spin density on the gallium center. Finally, time-dependent DFT revealed that in the paramagnetic derivatives, a set of pi-radical bands for β-HOMO(-N = 2−7) to SOMO (β-LUMO) transitions should be observed in the 590−830 nm range. For the mono-oxidized complex $(2)^{2+}$, an additional weak (oscillator strength, f, $\sim 10^{-3}$), low-energy intervalence charge transfer (IVCT) band for a β-HOMO-SOMO (β-LUMO, see Figure 5) transition was predicted to be found in

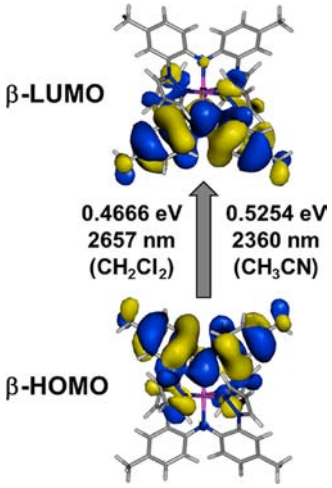

Figure 5. β-Frontier orbitals for $(2)^{2+}$ from TD-DFT calculations.

the NIR region. Moreover, the IVCT band was predicted to show a small solvent dependence, shifting (473 cm^{-1}) from 4237 cm^{-1} (2657 nm, $f = 6.3 \times 10^{-3}$) in CH_2Cl_2 to 3764 cm^{-1} (2360 nm, $f = 5.3 \times 10^{-3}$) in CH_3CN, in line with behavior expected for a Class II mixed valence species.

By careful choice of organic oxidants, it was possible to characterize and isolate either the one- or the two-electron oxidation products, $(2)^{2+}$ and $(3)^{3+}$, respectively, as mixed $SbCl_6^-/PF_6^-$ salts. For example, spectrophotometric titration of

dx.doi.org/10.1021/ic301437f | Inorg. Chem. 2012, 51, 12720−12728

$(CRET^+)(SbCl_6^-)$[29] ($E_{1/2}$ = 1.09 V versus Ag/AgCl, top of Figure 6) with substoichiometric amounts of $(\mathbf{1})(PF_6)$ in

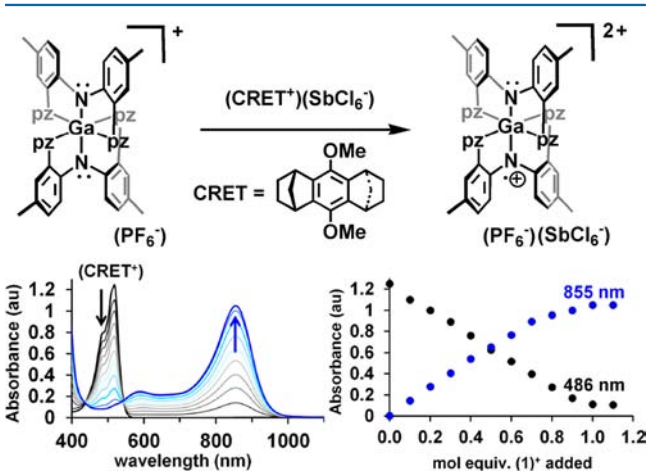

Figure 6. Preparation of $(\mathbf{2})(PF_6)(SbCl_6)$ and spectrophotometric titration using organic oxidant $(CRET^+)(SbCl_6^-)$.

CH_2Cl_2 showed the disappearance of the signature bands for the organic oxidant at 486 and 518 nm concomitant with the growth of new bands near 590 and 855 nm for pi-radical transitions of $(\mathbf{2})^{2+}$ [β-HOMO to SOMO]. The reaction was complete after an equimolar ratio of starting materials was achieved verifying the one-electron nature of oxidation of $(\mathbf{1})^+$. The shape and energies of these pi-radical bands are nearly identical to those found in the rhenium(I) or rhodium(III) complexes of this oxidized ligand.[24,25]

As indicated by the theoretical calculations, an IVCT band was predicted to be found in the NIR spectrum. For a weakly coupled Robin-Day Class II mixed valent species, the IVCT band is expected to have a Gaussian shape, be of weak intensity, and have an energy that is solvent dependent.[1c,3c,30] All of these expectations were met for the IVCT band of $(\mathbf{2})(PF_6)(SbCl_6)$. A representative spectrum for $(\mathbf{2})(PF_6)(SbCl_6)$ dissolved in CH_2Cl_2 is shown in Figure 7, while a summary of data obtained

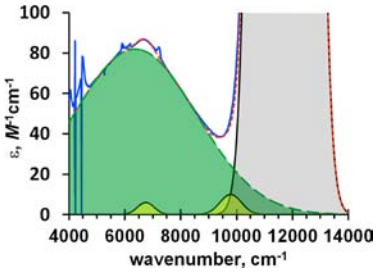

Figure 7. NIR spectrum (blue line) of $(\mathbf{2})(PF_6)(SbCl_6)$ in CH_2Cl_2 showing the IVCT band (green), the lowest energy pi-radical band (gray), and unidentified bands (yellow), and the sum of all Gaussian bands used to fit the spectra (red dotted line).

from multiple analyses using Gaussian fits of bands in three solvents (CH_2Cl_2, PC = propylene carbonate, CH_3CN) is given in Table 2. That is, the NIR spectra obtained for bulk samples of $(\mathbf{2})(PF_6)(SbCl_6)$ dissolved in various solvents revealed the presence of a very broad (full-width-at-half-maximum, $\Delta\tilde{\nu}_{1/2}$, ca. 5000 cm^{-1}), weak-intensity (ε_{max} ~ 40–80 $M^{-1}\,cm^{-1}$) IVCT band in the range of 6390–6925 cm^{-1} (green band in Figure 7). It is noteworthy that such a band is absent in the

Table 2. Summary of IVCT Band Shape Fitting and ET Parameters of $(\mathbf{2})(PF_6)(SbCl_6)$ in Three Different Solvents

	CH_2Cl_2	PC	CH_3CN
$E_{OP} = \lambda$ (cm^{-1})	6390 (±20)	6725 (±25)	6925 (±25)
ε_{max} ($M^{-1}\,cm^{-1}$)	79 (±3)	44 (±3)	55 (±5)
$\Delta\tilde{\nu}_{1/2}$ (cm^{-1})	5192 (±17)	4900 (±100)	4900 (±300)
oscillator strength[a], f_{obs} (f_{calc})	1.9×10^{-3} (6.3×10^{-3})	9.9×10^{-4} (n.d.)	1.2×10^{-3} (5.3×10^{-3})
H_{ab} (cm^{-1}), see eq 4	264	196	223
$\Delta\tilde{\nu}_{1/2}$ (HTL)[b]	3812	3910	3968
$\theta = \Delta\tilde{\nu}_{1/2}/\Delta\tilde{\nu}Z_{1/2}$ (HTL)	1.36	1.25	1.23
$\alpha = H_{ab}/\lambda$	0.0413	0.0291	0.0322
ΔG^* (cm^{-1}), see eq 5	1344	1491	1515
k_{et} (s^{-1}), see eq 6	2.9×10^{10}	7.6×10^{9}	8.6×10^{9}
$\gamma = 1/\varepsilon_s - 1/n^2$	0.382	0.480	0.582

[a] $f_{obs} = (4.6 \times 10^{-9})\varepsilon_{max}\Delta\tilde{\nu}_{1/2}$, f_{calc} from DFT calculations. [b] $\Delta\tilde{\nu}_{1/2}$ (HTL) = $[16\ln(2)k_BT\lambda]^{1/2}$ where k_B = 0.695 $cm^{-1}\,K^{-1}$ and T = 295 K.

NIR spectra of the doubly oxidized derivative $(\mathbf{3})^{3+}$ and of all $(L^{\bullet+})MXYZ$ complexes (M = Re^{I}, Rh^{III}) that contain only one singly oxidized ligand. It is also worthwhile to note that among the numerous reports on gallium(III) complexes of the type $[Ga(L^R)(L^{R\bullet})]^{n+}$ where L^R = a redox active ligand such as *N,N*-diazabutadiene = DAB[15] variants, di-*tert*-butyl semiquinone = DBSQ[18] or dbqdi,[21] an IVCT band has not been observed. Perhaps, the broadness and weak intensity of the IVCT band hinders its identification in these other systems. For $(\mathbf{2})(PF_6)$-$(SbCl_6)$, the Gaussian shape of the IVCT band and the indication of a Robin-Day Class II species from the analysis of K_{com} suggest that the Hush relations[31] (eqs 3 and 4) can be used to

$$E_{OP} = \lambda \tag{3}$$

$$H_{ab}\ (cm^{-1}) = [(4.2 \times 10^{-4})\varepsilon_{max}\Delta\tilde{\nu}_{1/2}E_{OP}]^{1/2}/d \tag{4}$$

estimate the strength of the electronic interaction. Here, E_{OP} is the energy of the absorption maximum, λ is the Marcus reorganization energy, H_{ab} is the electronic coupling element, ε_{max} is the molar extinction coefficient, $\Delta\tilde{\nu}_{1/2}$ is the full-width-at-half-maximum, and d is the separation between redox centers in Å. The value d = 3.9735 was used as this represents the distance between amido nitrogen centers obtained by taking into account an average of all crystallographic data for unoxidized, mono-oxidized, and dioxidized species in an effort to minimize potential errors of a single point structural determination. The following three observations further support that $(\mathbf{2})(PF_6)(SbCl_6)$ is a Robin-Day Class II(A) mixed valent species. First, from the Gaussian fits of the IVCT band, the experimental $\Delta\tilde{\nu}_{1/2}$ was larger than the theoretical value $\Delta\tilde{\nu}_{1/2}$ (HTL) = $[16\ln(2)k_BT\lambda]^{1/2}$.[3c,30] Second, as predicted by dielectric continuum theory, the energy of the IVCT band showed a linear correlation with the solvent parameter,[32] $\gamma = 1/\varepsilon_s - 1/n^2$ where ε_s is the static dielectric constant and n is the refractive index of the solvent (Figure S-4, Supporting Information). Third, the values of H_{ab} (ca. 200 cm^{-1}) and λ (6390–6925) cm^{-1} fall within the accepted limits of $0 < H_{ab} < \lambda/2$ or $0 < 2H_{ab}/\lambda < (1 - [\Delta\tilde{\nu}_{1/2}\ (HTL)]/2\lambda)$ for Class II or Class IIA species, respectively.[30] The thermal energy barrier to electron transfer, ΔG^*, calculated from classical Marcus Theory[33] (eq 5) is 1344–1515 cm^{-1}. The correspond-

dx.doi.org/10.1021/ic301437f | Inorg. Chem. 2012, 51, 12720–12728

ing rate constant for electron transfer k_{et} is found to be on the order of $(0.76-2.9) \times 10^{10}$ s^{-1} from eq 6, where Planck's constant, $h = 3.336 \times 10^{-11}$ $cm^{-1}\cdot s$,

$$\Delta G^* = (\lambda - 2H_{ab})^2/4\lambda \text{ cm}^{-1} \quad (5)$$

$$k_{et} = (2H_{ab}{}^2/h)[\pi^3/\lambda RT]^{1/2}\exp -(\Delta G^*/RT) \quad (6)$$

and the gas constant $R = 0.695$ cm^{-1} K^{-1}. These k_{et} values are comparable to those organic cation radicals with diarylamido groups linked by unsaturated 12- to 16-atom (phenylethynyl-) spacers but are of approximately 1−2 orders of magnitude smaller than found for shorter conjugated spacers such as in Figure 1A and their related *N,N′*-diphenyl-1,4-phenylenediamine cation radical counterparts.[34]

Figure 8 shows that the titration of $(OMN^+)(SbCl_6^-)$[35] ($E_{1/2}$ = 1.39 V versus Ag/AgCl) was complete after 1/2 equiv of

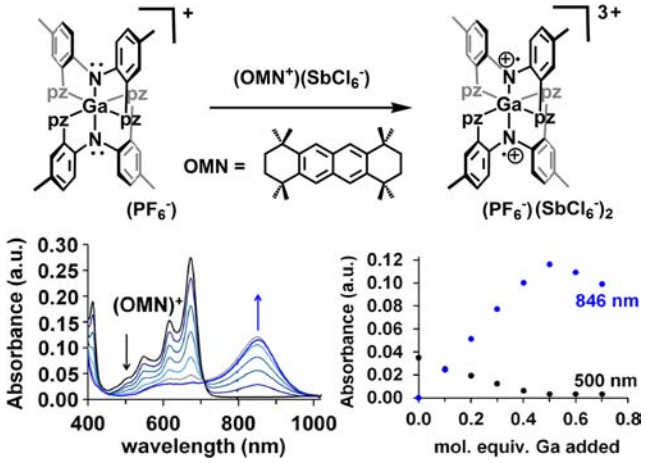

Figure 8. Spectrophotometric titration of $(3)(PF_6)(SbCl_6)_2$ and the organic oxidant $(OMN^+)(SbCl_6^-)$.

gallium complex was added to the oxidant verifying the two-electron nature of oxidation. In $(3)(PF_6)(SbCl_6)_2$, the pi-radical bands persisted in the electronic spectrum indicating a diradical species. The effective magnetic moment of the isolated powder, μ_{eff} = 2.4 μ_B (295 K), was lower than the expected spin-only value of 2.83 μ_B, which suggests that the triplet state is probably not wholly thermally populated. Although we do not have access to a magnetometer capable of variable (low) temperature magnetic measurements that would permit elucidation of the ground state properties, the theoretical calculations of $(3)^{3+}$ suggest that the singlet diradical lies 21.7 cm^{-1} lower than the triplet. This value is on par with the 23 cm^{-1} singlet−triplet energy difference in a tin(IV) complex of the aforementioned ONO-pincer radical ion, $Sn^{IV}(dbqdi)_2$,[21f] or the 64.6 cm^{-1} difference in Zn(tmeda)(3,6-DBSQ)(3,6-DBCat).[18b] The presence of a 'half-field' signal for a ΔM_s = 2 transition in the EPR spectra of solid $(3)(PF_6)(SbCl_6)_2$ acquired at 5 K in both normal and parallel-modes (Figure 9) verified that the triplet state is thermally populated even at this low temperature. It is noted that the EPR spectrum of an isolated sample of $(2)(PF_6)(SbCl_6)$ only showed an isotropic signal at g = 2.006, a g-value expected for a ligand-based radical; see Supporting Information.

It was possible to obtain X-ray quality, blue single crystals of the dioxidized complex $(3)(PF_6)_2(SbCl_6)\cdot 2.33CH_2Cl_2\cdot$toluene after mixing $(1)(PF_6)$ with 2 equiv of $(NO)(SbCl_6)$ in CH_2Cl_2,

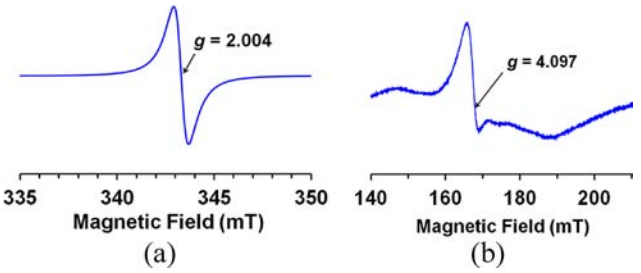

Figure 9. (a) X-band (9.63 GHz, 295 K) EPR spectrum of a powder sample of $(3)(PF_6)(SbCl_6)_2$, (b) 'half-field' spectrum acquired at 5 K (100 mW) in parallel-mode.

layering with toluene, and allowing solvents to diffuse. Obviously, solubility issues dictated the unexpected ratio of P- versus Sb-centered anions. After numerous attempts, X-ray quality violet crystals of "$[Ga(L)_2](PF_6)_{1.5}\cdot 1.05$ toluene$\cdot 0.65CH_2Cl_2\cdot 0.17H_2O$" were obtained from an equimolar mixture of $(1)(PF_6)$ with $(CRET)(SbCl_6)$ in CH_2Cl_2 layered with toluene, as above. After careful scrutiny of the various bond distances (vide infra), this latter structure is best described as the solvate of $[Ga(L^-)_2](PF_6)/[Ga(L^-)(L^0)](PF_6)_2$. An overlay of cation structures of $(1)^+$, $(2)^{2+}$, $(3)^{3+}$ and an intraligand bond labeling diagram are found in Figure 10.

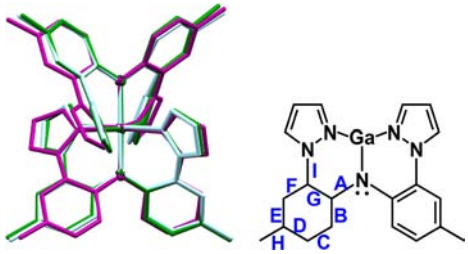

Figure 10. Left: Overlay of cation structures from X-ray diffraction. Key: pale blue, $(1)^+$; green, $(2)^{2+}$; purple, $(3)^{3+}$; right: Labeling diagram for bonds within the ligand.

Complete structural data are found in the Supporting Information. As suggested by calculations, the most significant structural changes along the valence series involved the Ga−N bond distances, which serve as oxidation number markers for the ligand. The average gallium-amido nitrogen Ga−N_{Ar} bond distance increased linearly from 1.947(3) Å in $[Ga^{III}(L^-)_2]^+$ to 2.023(5) Å in $[Ga^{III}(L^0)_2]^{3+}$ (0.074 Å change), while the average Ga−N_{pz} distance (dative bonds from the pyrazolyls) decreased from 2.102(3) Å in $[Ga^{III}(L^-)_2]^+$ to 2.039(5) Å in $[Ga^{III}(L^0)_2]^{3+}$ (0.063 Å change). As described earlier, each of these distances fall within ranges reported for other gallium(III) diphenylamido[26] or pyrazolyl[27] complexes. The bond length changes within the ligand backbone are much less pronounced, and are at the borderline of statistical significance. The most significant change occurs for bond-type G (right of Figure 10) between *ipso*- carbons which on average increases from 1.402(7) Å in $[Ga^{III}(L^-)_2]^+$ to 1.418(8) Å in $[Ga^{III}(L^0)_2]^{3+}$ (0.016 Å change). Such a change would imply a bonding interaction between these atoms in $(1)^+$, an interaction that is supported by computational studies.

In summary, the homoleptic complex $[Ga(L^-)_2](PF_6)$ and its mono- and dioxidized derivatives have been prepared and characterized in solution and in the solid state. The triplet state of the dioxidized species was found to be thermally populated

even at 5 K. For the paramagnetic, mono-oxidized species $(\mathbf{2})(PF_6)(SbCl_6)$, electrochemical and spectroscopic data established that weak electronic communication occurs between electroactive ligands across the gallium(III) bridge. The electronic communication across the diamagnetic metal ion bridge may occur either by direct tunneling,[33,36] by nonresonant charge transfer using the empty, high-energy 4p orbitals on gallium as a coupling medium (McConnell superexchange[37]), or by a thermally activated "hopping" mechanism.[38] Given the previous magnetic studies of diamagnetic metal complexes of organic diradicals that can promote either ferromagnetic or antiferromagnetic interactions with J values of different magnitude depending on the metal,[18b] the superexchange mechanism seems to be the most probable pathway for electronic communication. Clearly further experimental and theoretical investigations of other $[M(L)_2]^{n+}$ complexes of redox silent d^{10} or d^0 metal ions and their oxidized counterparts would be needed to elucidate the mechanism. Nevertheless, if oligomeric assemblies of the type LM-$[(L\text{-}L)M(L\text{-}L)]_n$-ML ($n$ = 0, 1, 2...) can be prepared then wire-like behavior is anticipated even for diamagnetic bridging ions. Stronger electronic communication is expected for transition metal analogues with available d-orbitals that can engage in $d\pi-p\pi$ interactions with the ligand. Details regarding such monomeric main group and transition metal complexes and their oligomeric assemblies will be reported in due course.

EXPERIMENTAL SECTION

General Considerations. The compounds Li(n-Bu) 1.6 M in hexanes, GaI_3, $TlPF_6$, $(NO)(SbCl_6)$ were purchased commercially and used as received. The compounds H(L),[24] $(CRET^+)(SbCl_6^-)$,[29] $(OMN^+)(SbCl_6^-)$[35] were prepared according to literature procedures. Solvents were dried by conventional means and distilled under nitrogen prior to use.

Physical Measurements. Midwest MicroLab, LLC, Indianapolis, Indiana 45250, performed all elemental analyses. Melting point determinations were made on samples contained in glass capillaries using an Electrothermal 9100 apparatus and are uncorrected. ^1H, ^{13}C, ^{19}F, and ^{31}P NMR spectra were recorded on a Varian 400 MHz spectrometer. Chemical shifts were referenced to solvent resonances at δ_H 5.33, δ_C 53.84 for CD_2Cl_2 or δ_H 1.94, δ_C 118.9 for CD_3CN and δ_H 2.05, δ_C 29.84 for acetone-d_6, while those for ^{19}F and ^{31}P NMR spectra were referenced against external standards of $CFCl_3$ (δ_F 0.00 ppm) and 85% H_3PO_4 (aq) (δ_P 0.00 ppm), respectively. Abbreviations for NMR and UV−vis br (broad), sh (shoulder), m (multiplet), ps (pseudo-), s (singlet), d (doublet), t (triplet), q (quartet), p (pentet), sept (septet). Electrochemical measurements were collected under a nitrogen atmosphere for samples as 0.1 mM solutions in CH_3CN and in CH_2Cl_2, each with 0.1 M NBu_4PF_6 as the supporting electrolyte. A three-electrode cell comprised of an Ag/AgCl electrode (separated from the reaction medium with a semipermeable polymer membrane filter), a platinum working electrode, and a glassy carbon counter electrode were used for the voltammetric measurements. Data were collected at scan rates of 50, 100, 200, 300, 400, and 500 mV/s. With this set up, the ferrocene/ferrocenium couple had an $E_{1/2}$ value of +0.53 V in CH_3CN and +0.41 V in CH_2Cl_2 at a scan rate of 200 mV/s, consistent with the literature values.[39] Solid state magnetic susceptibility measurements were performed using a Johnson-Matthey MSB-MK1 instrument. Electronic absorption (UV−vis/NIR) measurements were made on a Cary 5000 instrument. Emission spectra were recorded on a JASCO FP-6500 spectrofluorometer. EPR spectra were obtained on both solid powder samples and as solutions ~0.2 mM in 1:1 CH_2Cl_2/toluene mixtures using a Bruker ELEXYS E600 equipped with an ER4116DM cavity resonating at 9.63 GHz, an Oxford instruments ITC503 temperature controller and a ESR-900 helium flow cryostat. The spectra were recorded using 100 kHz field modulation unless otherwise specified.

Syntheses. *$[Ga(L)_2](I)$, $(\mathbf{1})(I)$.* A 3.45 mL aliquot of 1.6 M Li(n-Bu) in hexanes (5.52 mmol) was slowly added via syringe to a solution of 1.814 g (5.51 mmol) of H(L) in 15 mL of THF maintained at −78 °C. The resulting bright yellow solution was stirred 15 min, and then a solution of 1.241 g (2.76 mmol) of GaI_3 in 5 mL of THF was added by cannula transfer under nitrogen. The mixture was maintained at −78 °C for 2 h, and then the cold bath was removed and the mixture was allowed to warm naturally with stirring 12 h. The colorless precipitate (which exhibited bright blue luminescence upon irradiation with 354 nm light) was collected by vacuum filtration and was further dried under a vacuum 4 h to leave 2.026 g (86%) of $(\mathbf{1})(I)$ as a colorless powder. Anal. Calcd (obs.) for $C_{40}H_{36}N_{10}GaI$: C, 56.30 (56.22); H, 4.25 (4.27); N, 16.41 (16.19). ^1H NMR (acetone-d_6) δ_H: 8.40 (d, J = 2.6 Hz, 1H, H_5-pz), 7.28 (s, 1H, H_3−Ar), 7.22 (part of *AB*, 1H, Ar), 7.21 (d, J = 2.5 Hz, 1H, H_3pz), 7.09 (part of *AB*, 1H, Ar), 6.39 (*ps t*, J_{app} = 2.5 Hz, 1H, H_4pz), 2.25 (s, 3H, CH_3). ^{13}C NMR (acetone-d_6) δ_C: 143.8, 140.3. 132.9, 130.9, 130.7, 130.2, 127.2, 123.5, 108.3, 20.3. UV−vis (CH_2Cl_2): nm (ε, M^{-1} cm^{-1}) 249 (57,800), 267sh (32,300), 322 (24,700), 365 (19,300). Very fine needle crystals were grown by layering a CH_2Cl_2 solution with hexanes and then allowing solvents to slowly diffuse. A sample that was exposed to the atmosphere for a few hours analyzed as $(\mathbf{1})(I)\cdot H_2O$. Anal. Calcd (obs.) for $C_{40}H_{38}IGaN_{10}O$: C, 55.13 (55.62); H, 4.40 (4.27); N, 16.07 (15.56).

$[Ga(L)_2](PF_6)$, $(\mathbf{1})(PF_6)$. A 0.618 g (1.77 mmol) sample of $TlPF_6$ was added as a solid to a solution of 1.510 g (1.77 mmol) $(\mathbf{1})(I)$ in 20 mL of dichloromethane. After the mixture had been stirred magnetically 1 h, the colorless solution was separated from the pale yellow precipitate of TlI by filtration through a pad of Celite. The CH_2Cl_2 was removed under vacuum to give 1.52 g (99%) $(\mathbf{1})(PF_6)$ as a pale yellow powder. Mp: 280 °C dec Anal. Calcd (obs.) for $C_{40}H_{36}N_{10}F_6GaP$: C, 54.97 (55.37); H, 4.15 (4.25); N, 16.03 (15.82). ^1H NMR (acetone-d_6) δ: 8.34 (d, J = 2.6 Hz, 1H, H_5-pz), 7.25 (s, 1H, H_3−Ar), 7.22 (part of *AB*, 1H, Ar), 7.21 (d, J = 2.4 Hz, 1H, H_3pz), 7.09 (part of *AB*, 1H, Ar), 6.39 (*ps t*, J_{app} = 2.5 Hz, 1H, H_4pz), 2.24 (s, 3H, CH_3). ^{13}C NMR (acetone-d_6): 143.8, 140.3, 132.8, 130.9, 130.7, 130.2, 127.3, 123.4, 108.4, 20.3. ^{19}F NMR (acetone-d_6): δ_F −72.6 (d, J_{FP} = 707 Hz). ^{31}P NMR (acetone-d_6): δ_P −144.3 (sept, J_{P-F} = 707 Hz) ppm. UV−vis (CH_2Cl_2): nm (ε, M^{-1} cm^{-1}) 251 (47,500), 269sh (29,500), 323 (25,500), 366 (19,800). Single crystals of $(\mathbf{1})(PF_6)\cdot 1.75CH_2Cl_2$ used for X-ray diffraction were grown by layering a dichloromethane solution with hexanes and allowing solvents to slowly diffuse overnight.

Oxidation Reactions. *$[Ga(L)_2](PF_6)(SbCl_6)$, $(\mathbf{2})(PF_6)(SbCl_6)$.* A colorless solution of 0.1055 g (0.121 mmol) of $(\mathbf{1})(PF_6)$ in 10 mL of CH_2Cl_2 was added to a red solution of 0.0732 g (0.121 mmol) of $(CRET)(SbCl_6)$ in 25 mL of CH_2Cl_2. The flask originally containing $(\mathbf{1})(PF_6)$ was washed with another 10 mL of CH_2Cl_2 to ensure quantitative transfer to the reaction mixture. After the resulting royal blue solution had been stirred 15 min, solvent was removed under a vacuum. The resulting blue residue was washed with three 10 mL portions of hexanes to remove the organic byproduct and then was dried under a vacuum for several hours to leave 0.132 g (90%) of $(\mathbf{2})(PF_6)(SbCl_6)$ as a blue powder. μ_{eff} (solid, 295 K): 1.8 ± 0.1 μ_B. UV−vis (CH_2Cl_2): nm (ε, M^{-1} cm^{-1}) 250 (59,200), 321 (25,600), 362 (21,600), 596 (1,100), 857 (5,500), 1490 (90).

Violet needle crystals of $[Ga(L)_2](PF_6)_{1.5}\cdot 1.05$ toluene$\cdot 0.65CH_2Cl_2\cdot 0.17H_2O$ (see text) were grown by layering and equimolar mixture of $(\mathbf{1})(PF_6)$ and $(CRET)(SbCl_6)$ in CH_2Cl_2 with toluene and allowing solvents to diffuse in a −20 °C freezer.

$[Ga(L)_2](PF_6)(SbCl_6)_2$, $(\mathbf{3})(PF_6)(SbCl_6)_2$. A colorless solution of 0.1382 g (0.159 mmol) of $(\mathbf{1})(PF_6)$ in 20 mL of CH_2Cl_2 was added to a colorless solution of 0.1156 g (0.317 mmol) of $(NO)(SbCl_6)$ in 30 mL of CH_2Cl_2. After the resulting royal blue solution had been stirred 15 min, solvent was removed under a vacuum and the blue residue was dried under a vacuum to leave 0.213 g (87%) of $(\mathbf{3})(PF_6)(SbCl_6)_2$ as a blue powder. μ_{eff} (solid, 295 K): 2.4 ± 0.1 μ_B. UV−vis (CH_2Cl_2): nm (ε, M^{-1} cm^{-1}) 605 (1,300), 849 (6,200).

dx.doi.org/10.1021/ic301437f | Inorg. Chem. 2012, 51, 12720−12728

Table 3. Crystallographic data collection and structure refinement for $(1)(PF_6)\cdot 1.75CH_2Cl_2$, $(2)(PF_6)_{1.5}\cdot 1.05$ toluene$\cdot 0.65CH_2Cl_2\cdot 0.17H_2O$, and $(3)(PF_6)_2(SbCl_6)\cdot 2.33CH_2Cl_2\cdot$toluene

compound	$(1)(PF_6)\cdot 1.75CH_2Cl_2$	$(2)(PF_6)_{1.5}\cdot 1.05$ toluene$\cdot 0.65CH_2Cl_2\cdot 0.17H_2O$	$(3)(PF_6)_2(SbCl_6)\cdot 2.33CH_2Cl_2\cdot$toluene
formula	$C_{41.75}H_{39.50}Cl_{3.50}F_6GaN_{10}$	$C_{47.99}H_{45.68}Cl_{1.3}F_9GaN_{10}O_{0.17}P_{1.5}$	$C_{49.33}H_{48.66}Cl_{10.66}F_{12}GaN_{10}P_2Sb$
formula weight	1020.10	1098.43	1640.80
crystal system	triclinic	monoclinic	orthorhombic
space group	$P\bar{1}$	$P2_1/c$	$Pbca$
temp [K]	100(2)	100(2)	100(2)
a [Å]	12.9440(3)	17.6021(3)	17.5543(5)
b [Å]	17.4584(4)	24.6732(3)	24.9500(6)
c [Å]	20.9702(5)	23.2482(4)	29.1682(8)
α [°]	73.149(2)	90	90
β [°]	85.8230(10)	108.0987(18)	90
γ [°]	79.4170(10)	90	90
V [Å^3]	4457.29(18)	9597.2(3)	12775.1(6)
Z	4	8	8
D_{calcd} [g cm^{-3}]	1.520	1.520	1.706
λ [Å] (Mo or Cu Kα)	1.54178	1.54178	1.54178
μ.[mm^{-1}]	3.716	2.644	9.151
abs correction	numerical	numerical	numerical
$F(000)$	2078	4492	6526
θ range [°]	3.47−67.37	3.30−71.02	3.03−68.05
reflections collected	37225	53008	107137
independent reflections	14703 (R_{int} 0.0203)	18009 (R_{int} 0.0384)	11388 (R_{int} 0.0813)
T_min/max	0.4226/0.6243	0.68/0.963	0.2619/0.7110
data/restraints/parameters	14703/63/1231	18009/48/1285	11388/15/790
goodness-of-fit on F^2	0.982	0.914	1.062
R_1/wR_2 [$I > 2\sigma(I)$][a]	0.0484/0.1257	0.0433/0.1067	0.0646/0.1433
R_1/wR_2 (all data)[a]	0.0536/0.1294	0.0731/0.1163	0.0853/0.1528
largest diff peak/hole/e Å^{-3}	1.763/−0.730	0.84/−0.57	1.79/−1.28

[a] $R1 = \Sigma||F_o| - |F_c||/\Sigma|F_o|$ $wR^2 = [\Sigma w(|F_o| - |F_c|)^2/\Sigma w|F_o|^2]^{1/2}$.

Blue crystals of $(3)(PF_6)_2(SbCl_6)\cdot 2.33CH_2Cl_2\cdot$toluene were obtained from by mixing 15 mg (17 μmol) of $(1)(PF_6)$, 13 mg (34 μmol) of $(NO)(SbCl_6)$ in 5 mL of CH_2Cl_2, layering with 15 mL of toluene, and allowing solvents to diffuse.

Computational Studies. DFT calculations were performed with the M06 meta-hybrid GGA functional[40] using the def2-SV(P) double-ζ basis set.[41] Solvent (DCM) effects were accounted for by using the polarizable continuum model IEFPCM,[42] as implemented in Gaussian 09.[43] The chosen model proved superior over other combinations of functionals (M06 or B3LYP[44]) and basis sets (def2-SV(P) or 6311-G*/LANL2DZ[45]) for reproducing bond distances and spectroscopic data, as summarized in the Supporting Information. Gas phase structures of the metal complexes were optimized using the initial geometry from X-ray structural studies. Analytical vibrational frequency calculations were also carried out to verify that the optimized geometries were stationary points. Time-dependent DFT methodology was used for excitation energy calculations.[46]

Crystallography. X-ray intensity data from a colorless prism of $(1)(PF_6)\cdot 1.75CH_2Cl_2$ and a dark blue plate of $(3)(PF_6)_2(SbCl_6)\cdot 2.33CH_2Cl_2\cdot$toluene were collected at 100(2) K with a Bruker AXS 3-circle diffractometer equipped with a SMART2[47] CCD detector (Cu Kα radiation, λ = 1.54178 Å). X-ray intensity data from a violet needle of $(2)(PF_6)_{1.5}\cdot 1.05$ toluene$\cdot 0.65CH_2Cl_2\cdot 0.17H_2O$, were collected at 100(2) K with an Oxford Diffraction Ltd. Supernova equipped with a 135 mm Atlas CCD detector, by using Cu Kα radiation, λ = 1.54178 Å Raw data frame integration and Lp corrections were performed with SAINT+[47] for the data collected from the Bruker instrument but with CrysAlisPro[48] for that from the Oxford instrument. Final unit cell parameters were determined by least-squares refinement of 9343 reflections from the data set of $(1)(PF_6)\cdot 1.75CH_2Cl_2$, 19744 reflections from the data set of $(2)(PF_6)_{1.5}\cdot 1.05\cdot$toluene$\cdot 0.65CH_2Cl_2\cdot 0.17H_2O$, and 5460 reflections from data set of $(3)(PF_6)_2(SbCl_6)\cdot 2.33CH_2Cl_2\cdot$toluene, with $I > 2\sigma(I)$ for all cases. Analysis of the data showed negligible crystal decay during collection in each case. Direct methods structure solutions, difference Fourier calculations and full-matrix least-squares refinements against F^2 were performed with SHELXTL.[49] Numerical absorption corrections based on the real shapes of the crystals for $(1)(PF_6)\cdot 1.75CH_2Cl_2$, and $(3)(PF_6)_2(SbCl_6)\cdot 2.33CH_2Cl_2\cdot$toluene were applied using SADABS,[47] while an empirical absorption correction using spherical harmonics implemented in the SCALE3 ABSPACK scaling algorithm was used for $(2)(PF_6)_{1.5}\cdot 1.05\cdot$toluene$\cdot 0.65CH_2Cl_2\cdot 0.17H_2O$. The carbon atoms of the highly disordered solvent molecules in each structure were refined with isotropic displacement parameters. The remaining non-hydrogen atoms were refined with anisotropic displacement parameters. Hydrogen atoms were placed in geometrically idealized positions and included as riding atoms. The X-ray crystallographic parameters and further details of data collection and structure refinements are presented in Table 3.

■ ASSOCIATED CONTENT

Supporting Information

Emission spectrum, EPR spectra, structure diagrams including cif files, and computational details. This material is available free of charge via the Internet at http://pubs.acs.org.

■ AUTHOR INFORMATION

Corresponding Author

*Fax: 414-288-7066; tel: 414-288-3533; e-mail: james.gardinier@marquette.edu.

Notes

The authors declare no competing financial interest.

■ ACKNOWLEDGMENTS

J.R.G. thanks Prof. Rajendra Rathore for helpful suggestions and Prof. Qadir Timerghazin for assistance with theoretical calculations. J.R.G. thanks the NSF (CHE-0848515) for financial support. Funds for EPR spectroscopic studies (Grant NIH-RR001980) are gratefully acknowledged. This research was also funded in part by National Science Foundation awards OCI-0923037 "MRI: Acquisition of a Parallel Computing Cluster and Storage for the Marquette University Grid (MUGrid)" and CBET-0521602 "Acquisition of a Linux Cluster to Support College-Wide Research & Teaching Activities."

■ REFERENCES

(1) (a) Isied, S. S., Ed. *Electron Transfer Reactions: Inorganic, Organometallic, and Biological Applications*; Advances in Chemistry Series 253; American Chemical Society: Washington, DC, 1997. (b) Prassides, K., Ed. *Mixed Valency Systems: Applications in Chemistry, Physics and Biology*; Kluwer Academic Publishers: Dordrecht, 1991. (c) Robin, M. B.; Day, P. *Adv. Inorg. Chem. Radiochem.* **1967**, *10*, 247−422.

(2) (a) Kaim, W.; Lahiri, G. K. *Angew. Chem., Int. Ed.* **2007**, *46*, 1778−1796. (b) Kaim, W.; Klein, A.; Glöckle, M. *Acc. Chem. Res.* **2000**, *33*, 755−763. (c) Glover, S. D.; Goeltz, J. C.; Lear, B. J.; Kubiak, C. P. *Eur. J. Inorg. Chem.* **2009**, 585−594.

(3) (a) Creutz, C.; Taube, H. *J. Am. Chem. Soc.* **1969**, *91*, 3988−3989. (b) Creutz, C.; Taube, H. *J. Am. Chem. Soc.* **1973**, *95*, 1086−1094. (c) Crutchley, R. J. *Adv. Inorg. Chem.* **1994**, *41*, 273−325.

(4) (a) Heckmann, A.; Lambert, C. *Angew. Chem., Int. Ed.* **2012**, *51*, 326−392. (b) Hankache, J.; Wenger, O. S. *Chem. Rev.* **2011**, *111*, 5138−5178.

(5) (a) Nelsen, S. F.; Tran, H. Q.; Nagy, M. A. *J. Am. Chem. Soc.* **1998**, *120*, 298−304. (b) Szeghalmi, A. V.; Erdmann, M.; Engel, V.; Schmitt, M.; Amthor, S.; Kriegisch, V.; Nöll, G.; Stahl, R.; Lambert, C.; Leusser, D.; Stalke, D.; Zabel, M.; Popp, J. *J. Am. Chem. Soc.* **2004**, *126*, 7834−7845. (c) Lambert, C.; Nöll, G. *J. Am. Chem. Soc.* **1999**, *121*, 8434−8442. (d) Coropceanu, V.; Malagoli, M.; André, J. M.; Brédas, J. L. *J. Am. Chem. Soc.* **2002**, *124*, 10519−10530. (e) Coropceanu, V.; Gruhn, N. E.; Barlow, S.; Lambert, C.; Durivage, J. C.; Bill, T. G.; Nöll, G.; Marder, S. R.; Brédas, J. L. *J. Am. Chem. Soc.* **2004**, *126*, 2727−2731. (f) Lambert, C.; Risko, C.; Coropceanu, V.; Schelter, J.; Amthor, S.; Gruhn, N. E.; Durivage, J. C.; Brédas, J. L. *J. Am. Chem. Soc.* **2005**, *127*, 8508−8516. (g) Yano, M.; Ishida, Y.; Aoyama, K.; Tatsumi, M.; Sato, K.; Shiomi, D.; Ichimura, A.; Takui, T. *Synth. Met.* **2003**, *137* (1−3), 1275−1276. (h) Plater, M. J.; Jackson, T. *J. Chem. Soc., Perkin Trans. 1* **2001**, *20*, 2548−2552. (i) Low, P. J.; Paterson, M. A. J.; Yufit, D. S.; Howard, J. A. K.; Cherryman, J. C.; Tackley, D. R.; Brook, R.; Brown, B. *J. Mater. Chem.* **2005**, *15*, 2304−2315. (j) Bonvoisin, J.; Launay, J. −P.; Van der Auweraer, M.; De Schryver, F. C. *J. Phys. Chem.* **1994**, *98*, 5052−5057.

(6) (a) Rohde, D.; Dunsch, L.; Tabet, A.; Hartmann, H.; Fabian, J. *J. Phys. Chem. A* **2006**, *110*, 8223−8231. (b) Odom, S. A.; Lancaster, K.; Beverina, L.; Lefler, K. M.; Thompson, N. J.; Coropceanu, V.; Bredas, J. −L.; Marder, S. R.; Barlow, S. *Chem.—Eur. J.* **2007**, *13*, 9637−9646. (c) Lacroix, J. C.; Chane-Ching, K. I.; Maquère, F.; Maurel, F. *J. Am. Chem. Soc.* **2006**, *128*, 7264−7276.

(7) (a) Lambert, C.; Nöll, G.; Schelter, J. *Nat. Mater.* **2002**, *1*, 69−73. (b) Lambert, C.; Nöll, G. *J. Chem. Soc., Perkin Trans. 2* **2002**, 2039−2043.

(8) Jones, S. C.; Coropceanu, V.; Barlow, S.; Kinnibrugh, T.; Timofeeva, T.; Brédas, J. −L.; Marder, S. R. *J. Am. Chem. Soc.* **2004**, *126*, 11782−11783.

(9) Nöll, G.; Avola, M. *J. Phys. Org. Chem.* **2006**, *19*, 238−241.

(10) See also: (a) Sun, D.; Lindeman, S. V.; Rathore, R.; Kochi, J. K. *J. Chem. Soc. Perkin Trans. 2* **2001**, 1585−1594. (b) Rosokha, S. V.; Sun, D.-L.; Kochi, J. K. *J. Phys. Chem. A* **2002**, *106*, 2283−2292. (c) Lindeman, S. V.; Rosokha, S. V.; Sun, D.; Kochi, J. K. *J. Am. Chem. Soc.* **2002**, *124*, 843−855.

(11) Examples with inorganic/organometallic donors and bridges are also known such as: (a) {(terpyRu)(μ-terpy-$(C_2)_n$-Fc_m-$(C_2)_n$-terpy)[Ru(terpy)]$^{5+}$ (n = 0, 1; Fc = ferrocenyl, m = 1−3) Dong, T.-Y.; Lin, H.-Y.; Lin, S.-F.; Huang, C.-C.; Wen, Y.-S.; Lee, L. *Organometallics* **2008**, *27*, 555−562 and references. Polyferrocene examples: (b) Cowan, D. O.; Levanda, C.; Park, J.; Kaufman, F. *Acc. Chem. Res.* **1973**, *6*, 1−7. (c) Le Vanda, C.; Bechard, K.; Cowan, D. O.; Rausch, M. D. *J. Am. Chem. Soc.* **1977**, *99*, 2964−2968. (d) Dong, T.-Y.; Lee, W.-Y.; Su, P.-T.; Chang, L.-S.; Lin, K.-J. *Organometallics* **1998**, *17*, 3323−3330. (e) Dong, T.-Y.; Lee, S. H.; Chang, C. K.; Lin, H. M.; Lin, K. J. *Organometallics* **1997**, *16*, 2773−2786. (f) Brown, G. M.; Meyer, T. J.; Cowan, D. O.; LeVanda, C.; Kaufman, F.; Roling, R. V.; Raush, M. D. *Inorg. Chem.* **1975**, *14*, 506−511. (g) Cowan, D. O.; Kaufman, F. *J. Am. Chem. Soc.* **1970**, *92*, 219−220. (h) Scheibitz, M.; Heilmann, J. B; Winter, R. F; Bolte, M.; Bats, J. W.; Wagner, M. *Dalton Trans.* **2005**, *1*, 159−170.

(12) (a) Dei, A.; Sorace, L. *Appl. Magn. Reson.* **2010**, *38*, 139−153. (b) Zanello, P.; Corsini, M. *Coord. Chem. Rev.* **2006**, *250* (15 + 16), 2000−2022. (c) Pierpont, C. G. *Coord. Chem. Rev.* **2001**, *216*, 99−125. (d) Pierpont, C. G.; Lange, C. W. *Prog. Inorg. Chem.* **1994**, *41*, 331−442.

(13) Eisenberg, R.; Gray, H. B. *Inorg. Chem.* **2011**, *50*, 9741−9751.

(14) Quinone diimines: (a) Moriuchi, T.; Hirao, T. *Acc. Chem. Res.* **2012**, *45*, 347−360. (b) Uhlig, E. *Pure Appl. Chem.* **1988**, *60*, 1235−1240. (c) Vrieze, K.; Van Koten, G. *Inorg. Chim. Acta* **1985**, *100*, 79−96. (d) Balch, A. L.; Holm, R. H. *J. Am. Chem. Soc.* **1966**, *88*, 5201−5208.

(15) DAB complexes: (a) Tuononen, H. K.; Armstrong, A. F. *Dalton Trans.* **2006**, 1885−1894. (b) Baker, R. J.; Jones, C.; Mills, D. P.; Murphy, D. M.; Hey-Hawkins, E.; Wolf, R. *Dalton Trans.* **2006**, 64−72. (c) Tuononen, H. K.; Armstrong, A. F. *Inorg. Chem.* **2005**, *44*, 8277−8284. (d) Baker, R. J.; Farley, R. D.; Jones, C.; Mills, D. P.; Kloth, M.; Murphy, D. M. *Chem.—Eur. J.* **2005**, *11*, 2972−2982. (e) Baker, R. J.; Jones, C.; Kloth, M.; Platts, J. A. *Angew. Chem., Int. Ed.* **2003**, *42*, 2660−2663. (f) Pott, T.; Jutzi, P.; Kaim, W.; Schoeller, W. W.; Neumann, B.; Stammler, H. −G.; Wanner, M. *Organometallics* **2002**, *21*, 3169−3172. (g) Rijnberg, E.; Richter, B; Thiele, K. H.; Boersma, J.; Veldman, N.; Spek, A. L.; van Koten, G. *Inorg. Chem.* **1998**, *37*, 56−63. (h) Gardiner, M. G.; Raston, C. L.; Skelton, B. W.; White, A. H. *Inorg. Chem.* **1997**, *36*, 2795−2803. (i) Gardiner, M. G.; Hanson, G. R.; Henderson, M. J.; Lee, F. C.; Raston, C. L. *Inorg. Chem.* **1994**, *33*, 2456−2461.

(16) β-Diketiminatos: (a) Tsai, Y.-C. *Coord. Chem. Rev.* **2012**, *256* (5−8), 722−758. (b) Macedo, F. P.; Gwengo, C.; Lindeman, S. V.; Smith, M. D.; Gardinier, J. R. *Eur. J. Inorg. Chem.* **2008**, *20*, 3200−3211.

(17) Pyridine-diimines: (a) Sieh, D.; Schlimm, M.; Andernach, L.; Angersbach, F.; Nueckel, S.; Schoeffel, J.; Susnjar, N.; Burger, P. *Eur. J. Inorg. Chem.* **2012**, *3*, 444−462. (b) Zhu, D.; Thapa, I.; Korobkov, I.; Gambarotta, S.; Budzelaar, P. H. M. *Inorg. Chem.* **2011**, *50*, 9879−9887. (c) Myers, T. W.; Berben, L. A. *J. Am. Chem. Soc.* **2011**, *133*, 11865−11867. (d) Myers, T. W.; Kazem, N.; Stoll, S.; Britt, R. D.; Shanmugam, M.; Berben, L. A. *J. Am. Chem. Soc.* **2011**, *133*, 8662−8672.

(18) (a) Pierpont, C. G. *Inorg. Chem.* **2011**, *50*, 9766−9772. (b) Lange, C. W.; Conklin, B. J.; Pierpont, C. G. *Inorg. Chem.* **1994**, *33*, 1276−1283. (c) Adams, D. M.; Dei, A.; Hendrickson, D. N.; Rheingold, A. L. *Angew. Chem., Int. Ed. Engl.* **1993**, *32*, 391−392.

(19) (a) Chaudhuri, P.; Wagner, R.; Pieper, U.; Biswas, B.; Weyhermuller, T. *Dalton Trans.* **2008**, 1286−1288. (b) Verani, C. N.; Gallert, S.; Bill, E.; Weyhermüller, T.; Weighardt, K.; Chaudhuri, P. *Chem. Commun.* **1999**, 1747−1748.

(20) (a) Scarborough, C. C.; Sproules, S.; Doonan, C. J.; Hagen, K. S.; Weyhermuller, T.; Weighardt, K. *Inorg. Chem.* **2012**, *51*, 6969−6982. (b) Scarborough, C. C.; Lancaster, K. M.; DeBeer, S.; Weyhermüller, T.; Sproules, S.; Wieghardt, K. *Inorg. Chem.* **2012**, *51*, 3718−3732 and references.

(21) (a) Szigethy, G.; Heyduk, A. F. *Dalton Trans.* **2012**, *41*, 8144−8152. (b) Brown, M. A.; El-Hadad, A. A.; McGarvey, B. R.; Sung, R. C. W.; Trikha, A. K.; Tuck, D. G. *Inorg. Chim. Acta* **2000**, *300*−*302*, 613−621. (c) Chaudhury, P.; Hess, M.; Hildenbrand, K.; Bill, E.; Weyhermüller, T.; Wieghardt, K. *Inorg. Chem.* **1999**, *38*, 2781−2790. (d) Camacho-Camacho, C.; Merino, G.; Martínez-Martínez, F. J.; Nöth, H.; Contreras, R. *Eur. J. Inorg. Chem.* **1999**, 1021−1027. (e) Brown, M. A.; Castro, J. A.; McGarvey, B. R.; Tuck, D. G. *Can. J. Chem.* **1999**, *77*, 502−510. (f) Bencini, A.; Ciofini, I.; Giannasi, E.; Daul, C. A.; Doclo, K. *Inorg. Chem.* **1998**, *37*, 3719−3725.

(22) Forum on Redox-Active Ligands: *Inorg. Chem.* **2011**, *50*, 9737−9914

(23) Other recent reviews: (a) Kaim, W. *Eur. J. Inorg. Chem.* **2012**, *3*, 343−348. (b) Lyaskovskyy, V.; de Bruin, B. *ACS Catalysis* **2012**, *2*, 270−279. (c) Kaim, W. *Inorg. Chem.* **2011**, *50*, 9752−9765. (d) Kaim, W.; Schwederski, B. *Coord. Chem. Rev.* **2010**, *254* (13−14), 1580−1588. (e) Ray, K.; Petrenko, T.; Wieghardt, K.; Neese, F. *Dalton Trans.* **2007**, 1552−1566. (f) Evangelio, E.; Ruiz-Molina, D. *Eur. J. Inorg. Chem.* **2005**, *15*, 2957−2971. (g) Hirao, T. *Coord. Chem. Rev.* **2002**, *226* (1−2), 81−91.

(24) (a) Wanniarachchi, S.; Liddle, B. J.; Toussaint, J.; Lindeman, S. V.; Bennett, B.; Gardinier, J. R. *Dalton Trans.* **2011**, *40*, 8776−8787. (b) Wanniarachchi, S.; Liddle, B. J.; Toussaint, J.; Lindeman, S. V.; Bennett, B.; Gardinier, J. R. *Dalton Trans.* **2010**, *39*, 3167−3169.

(25) (a) Wanniarachchi, S.; Liddle, B. J.; Kizer, B.; Hewage, J.; Bennett, B.; Lindeman, S. V.; Gardinier, J. R. *Inorg. Chem.* **2012**, *50*, 10572−10580. (b) Wanniarachchi, S.; Liddle, B. J.; Lindeman, S. V.; Gardinier, J. R. *J. Organomet. Chem.* **2011**, *696*, 3623−3636.

(26) Niemeyer, M.; Goodwin, T. J.; Risbud, S. H.; Power, P. P. *Chem. Mater.* **1996**, *8*, 2745−2750.

(27) (a) Yurkerwich, K.; Parkin, G. *J. Clust. Sci.* **2010**, *21*, 225−234. (b) Reger, D. L.; Ding, Y. *Organometallics* **1993**, *12*, 4485−4492. (c) Cowley, A. H.; Carrano, C. J.; Geerts, R. L.; Jones, R. A.; Nunn, C. M. *Angew. Chem., Int. Ed. Engl.* **1988**, *27*, 277−278.

(28) (a) Zanello, P. *Inorganic Electrochemistry: Theory, Practice and Applications*; Royal Society of Chemistry: Cambridge, 2003; pp 174−178. (b) Astruc, D. *Electron Transfer and Radical Processes in Transition-Metal Chemistry*; VCH Publishers, Inc.: New York, 1995; pp 34−36.

(29) Rathore, R.; Burns, C. L.; Deselinescu, M. I.; Denmark, S. E.; Bui, T. *Org. Synth.* **2005**, *82*, 1−9.

(30) Brunschwig, B. S.; Creutz, C.; Sutin, N. *Chem. Soc. Rev.* **2002**, *31*, 168−184.

(31) (a) Hush, N. S. *Prog. Inorg. Chem.* **1967**, *8*, 391−444. (b) Hush, N. S. *Coord. Chem. Rev.* **1985**, *64*, 135−157.

(32) (a) Abbott, A. P.; Rusling, J. F. *J. Phys. Chem.* **1990**, *94*, 8910−8912. (b) Brunschwig, B. S.; Ehrenson, S.; Sutin, N. *J. Phys. Chem.* **1986**, *90*, 3657−3668.

(33) Marcus, R. A.; Sutin, N. *Biochim. Biophys. Acta* **1985**, *811*, 265−322. (b) Sutin, N. *Prog. Inorg. Chem.* **1983**, *30*, 441−499.

(34) Nishiumi, T.; Nomura, Y.; Chimoto, Y.; Higuchi, M.; Yamamoto, K. *J. Phys. Chem. B.* **2004**, *108*, 7992−8000.

(35) (a) Le Maguerès, P.; Lindeman, S. V.; Kochi, J. K. *Org. Lett.* **2000**, *2*, 3567−357. (b) Rathore, R.; Kochi, J. K. *Acta Chem. Scand.* **1998**, *52*, 114−130. (c) Bruson, H. A.; Kroeger, J. W. *J. Am. Chem. Soc.* **1940**, *62*, 36−44.

(36) (a) Weiss, E. A.; Kriebel, J. K.; Rampi, M. A.; Whitesides, G. M. *Phil. Trans. R. Soc. A* **2007**, *365*, 1509−1537. (b) Albinsson, B.; Eng, M. P.; Pettersson, K.; Winters, M. U. *Phys. Chem. Chem. Phys.* **2007**, *9*, 5847−5864.

(37) (a) Petrov, E. G.; May, A. *J. Phys. Chem. A* **2001**, *105*, 10176−10186. (b) Onipko, A. *Chem. Phys. Lett.* **1998**, *292*, 267−272. (c) Lopez-Castillo, J. −M.; Jay-Gerin, J. −P. *J. Phys. Chem.* **1996**, *100*, 14289−14297. (d) Naleway, C. A.; Curtiss, L. A.; Miller, J. R. *J. Phys. Chem.* **1991**, *95*, 8434−8437. (e) McConnell, H. M. *J. Chem. Phys.* **1961**, *35*, 508−515.

(38) (a) Berlin, Y. A.; Hutchison, G. R.; Rempala, P.; Ratner, M. A.; Michl, J. *J. Phys. Chem. A* **2003**, *107*, 3970−3980. (b) Berlin, Y. A.; Burin, A. L.; Ratner, M. A. *Chem. Phys.* **2002**, *275*, 61−74 (b).

(39) (a) Gagné, R. R.; Koval, C. A.; Lisensky, G. C. *Inorg. Chem.* **1980**, *19*, 2855−2857. (b) Noviandri, I.; Brown, K. N.; Fleming, D. S.; Gulyas, P. T.; Lay, P. A.; Masters, A. F.; Phillips, L. *J. Phys. Chem. B* **1999**, *103*, 6713−6722. (c) Bond, A. M.; Oldham, K. B.; Snook, G. A. *Anal. Chem.* **2000**, *72*, 3492−3496. (d) Bao, D.; Millare, B.; Xia, W.; Steyer, B. G.; Gerasimenko, A. A.; Ferreira, A.; Contreras, A.; Vullev, V. I. *J. Phys. Chem. A* **2009**, *113*, 1259−1267.

(40) Zhao, Y.; Truhlar, D. G. *Theor. Chem. Acc.* **2008**, *120*, 215−241.

(41) Weigend, F.; Ahlrichs, R. *Phys. Chem. Chem. Phys.* **2005**, *7*, 3297−3305.

(42) Scalmani, G.; Frisch, M. J. *J. Chem. Phys.* **2010**, *132*, 114110−114124.

(43) Gaussian 09, Revision B.01, Frisch, M. J.; Trucks, G. W.; Schlegel, H. B.; Scuseria, G. E.; Robb, M. A.; Cheeseman, J. R.; Scalmani, G.; Barone, V.; Mennucci, B.; Petersson, G. A.; Nakatsuji, H.; Caricato, M.; Li, X.; Hratchian, H. P.; Izmaylov, A. F.; Bloino, J.; Zheng, G.; Sonnenberg, J. L.; Hada, M.; Ehara, M.; Toyota, K.; Fukuda, R.; Hasegawa, J.; Ishida, M.; Nakajima, T.; Honda, Y.; Kitao, O.; Nakai, H.; Vreven, T.; Montgomery, Jr., J. A.; Peralta, J. E.; Ogliaro, F.; Bearpark, M.; Heyd, J. J.; Brothers, E.; Kudin, K. N.; Staroverov, V. N.; Kobayashi, R.; Normand, J.; Raghavachari, K.; Rendell, A.; Burant, J. C.; Iyengar, S. S.; Tomasi, J.; Cossi, M.; Rega, N.; Millam, J. M.; Klene, M.; Knox, J. E.; Cross, J. B.; Bakken, V.; Adamo, C.; Jaramillo, J.; Gomperts, R.; Stratmann, R. E.; Yazyev, O.; Austin, A. J.; Cammi, R.; Pomelli, C.; Ochterski, J. W.; Martin, R. L.; Morokuma, K.; Zakrzewski, V. G.; Voth, G. A.; Salvador, P.; Dannenberg, J. J.; Dapprich, S.; Daniels, A. D.; Farkas, Ö.; Foresman, J. B.; Ortiz, J. V.; Cioslowski, J.; Fox, D. J. Gaussian, Inc., Wallingford CT, 2009.

(44) (a) Becke, A. D. *J. Chem. Phys.* **1993**, *98*, 5648−5652. (b) Lee, C.; Yang, W.; Parr, R. G. *Phys. Rev. B* **1988**, *37*, 785−789.

(45) (a) Hay, P. J.; Wadt, W. R. *J. Chem. Phys.* **1985**, *82*, 270−283. (b) Wadt, W. R.; Hay, P. J. *J. Chem. Phys.* **1985**, *82*, 284−298. (c) Hay, P. J.; Wadt, W. R. *J. Chem. Phys.* **1985**, *82*, 299−310.

(46) (a) Casida, M. E.; Jamorski, C.; Casida, K. C.; Salahub, D. R. *J. Chem. Phys.* **1998**, *108*, 4439−4449. (b) Scalmani, G.; Frisch, M. J.; Mennucci, B.; Tomasi, J.; Cammi, R.; Barone, V. *J. Chem. Phys.*, **2006**, *124*, 094107: 1-15.

(47) *SMART APEX2 Version 2.1−4, SAINT+ Version 7.23a and SADABS Version 2004/1*; Bruker Analytical X-ray Systems, Inc.: Madison, Wisconsin, USA, 2005.

(48) *CrysAlisPro*, Version 1.171.34.46; Agilent Technologies: Santa Clara, CA, 2010, (release 25−11−2010 CrysAlis171 .NET), (compiled Nov 25 2010, 17:55:46)

(49) Sheldrick, G. M. *SHELXTL*, Version 6.12; Bruker Analytical X-ray Systems, Inc.: Madison Wisconsin, USA, 2001.